Power Density Limit for Stable Optical Trapping of a Single Microcluster of Calix[4]arene in Water

Nur Izzati Mahadi
Shahrul Kadri Ayop
Muhammad Safuan Mat Yeng
Faridah Lisa Supian

DOI: https://doi.org/10.37178/ca-c.21.5.081

Nur Izzati Mahad*, Department of Physics, Faculty of Science and Mathematics, Sultan Idris Education University, 35900 Tanjong Malim, Perak, Malaysia*

Shahrul Kadri Ayop, *Department of Physics, Faculty of Science and Mathematics,Sultan Idris Education University,35900 Tanjong Malim, Perak, Malaysia*
Email: shahrul.kadri@fsmt.upsi.edu.my

Muhammad Safuan Mat Yeng*, Department of Physics, Faculty of Science and Mathematics,Sultan Idris Education University, 35900 Tanjong Malim, Perak, Malaysia*

Faridah Lisa Supian, *Department of Physics****,*** *Faculty of Science and Mathematics,Sultan Idris Education University, 35900 Tanjong Malim, Perak, Malaysia*

Abstract

This study aimed to determine the upper and lower limit of optical power density for the purpose of stable optical trapping of a single microcluster of Calix[4]arene in water. Various sizes of the microcluster (effective radius of 0.5 µm to 2.75 µm) were optically trapped using optical tweezers at 976 nm in deionized water (DIW). The optical stiffness of the optical trap is evaluated by determining the corner frequency from the power spectral density analysis of the microcluster trajectory. It has been found that the minimum power density required for the optical trapping of a single microcluster, regardless of the size of the microcluster, is 0.69 MW/cm^2. However, the maximum power density for stable trapping varies with the size of the microcluster. The finding provides a starting point for possible optically controlled calixarene microcluster for nanosensor applications in water.

Keywords*: Optical tweezers, calixarene, microcluster, optical trapping*

Introduction

Arthur Ashkin was the first to established Optical Tweezers (OT) in his research in 1970, for which he was awarded a noble prize in 2018 [1]. Recently, the usage of OT has widely spread into a lot of different research fields like physics [2], chemistry[3], molecular biology [4], medicine[5], agriculture[6], and others. Many researchers are interested in using OT nowadays because of the unique characteristics that can trap and manipulate single nano and micro-scale particles without any physical contact and only use a highly focused laser beam to trap and manipulate the particles[7, 8]. A traditional method to hold particles physically, such as micropipette or Atomic Force Microscopy (AFM), can damage the delicate sample[9]. Additionally, optical trapping studies using OT can be done in the different surrounding mediums, either in the air

[10], vacuum [11], or liquid[12], making it more desirable for the researcher to use OT in their research. However, most researchers focus on trapping a single spherical particle rather than a single irregular shaped particle cluster, whether in an air medium or liquid medium.

On the other hand, the optical manipulation by trapping an irregular shape particle cluster is rather interesting because of the possibility of broadening the trapping range [13]. So, this study reports the trapping of a single irregular shape microcluster of Calix[4]arene in a water medium. Calixarene is a functional molecule that poses wide potential applications as nanoprobes or nanosensors[14]. The most important part of the OT system is to have stable optical trapping of a particle under investigation. It is crucial for stable optical trapping of particles to set a suitable optical power density [15]. If the optical power density was set too high, the particle's probability of being pushed away from the laser focus point is relatively high. On the other hand, if the optical power density was set too low, the particle could not be trapped.

To justify whether the power density is too low or too high for stable optical trapping, we can measure the optical stiffness, k_T, of the trapped particle. The optical stiffness is evaluated by determining the corner frequency, f_c, from the power spectral density (PSD) of the particle's trajectory obtained from a quadrant photodiode detector (QPD). The f_c parameter has been utilized to study the red blood cell [[16], to differentiate between a normal or an affected red blood cell [17], to observe the temperature rise at the optical trap centre[18], and to recognize the structure and dynamics of the coagulation of clusters [18]. The relationship between k_T and f_c is shown by Equation (1).

$$k_T = 2\pi\gamma_0 f_c \tag{1}$$

where $\gamma_0 = 6\pi\eta r$, η is the viscosity of the surrounding medium, and r is the radius of the spherical shape of the trapped particle. However, for irregular shape particles, the effective size r^* is used. r^* is approximated by taking the average of half orthogonal lengths of the particle as expressed in Equation (2).

$$r^* = \frac{1}{2}\left(\frac{l_x}{2} + \frac{l_y}{2}\right) \tag{2}$$

where l_x and l_y is the particle length along x and y-axes perpendicular to the laser propagation direction.

Literature Review

Particles with irregular shapes can be optically trapped primarily in the air as the surrounding medium [19, 20]. The previous researchers reported that radiation and photophoretic forces were responsible for the trap generated from a single focused laser beam[20, 21]. However, trapping a particle in an air medium poses some challenges. In particular, they have to wait for the particle to fall into the trap rather than seek it or push the particle away from the laser focus point because of the vast scattering force [22, 23]. On the other hand, trapping in a liquid medium is beneficial because of higher viscosity, allowing for a higher drag force that can temporarily hold the particle before falling into the trap. In addition, liquid has a higher refractive index than air, increasing the scattering force, thus making a weak optical trapping [24]. Furthermore, a higher relative refractive index produces a more significant scattering force, which pushes particles away from the laser focal point.

A stable and strong optical trap can be justified by finding the value of the optical stiffness of the trap system [21]. Other than the surrounding medium of the trapped particle, the optical power density from the used laser power also affects the value of k_T [14]. Therefore, it is crucial to determine the power density limit to set up the stable optical trapping of the particles. This paper reports the power density limit for stable

optical trapping of a single microcluster of Calix[4[arene in deionized water.

Material and Method

Calixarene is an organic material that possesses a cratershaped nanostructure , as in Figure 1(a). It has various unique characteristics commonly applied in advanced materials, biotechnology, and nanosensors . Calixarene is well-known for the host-guest substance; thus, several studies have been carried out on cation sensors [25-27]. Calix[4]arene that is being used in this study is Calix[4]arene-25,26,27,28-tetrol, which is comprised of four phenolic units as in Figure 1(b).

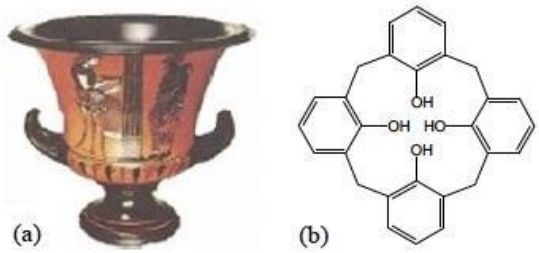

Figure 1. Calixarene, a host-guest substance: (a) Calix cratershaped. (b) Calix[4]arene-25,26,27,28-tetrol comprised of four phenolic units. Calixarene used in this work. (Source: *[25-27]*).

The microcluster of Calix[4]arene sample was prepared by mixing 1.7 mg of pure Calix arene powder (Sigma Aldrich) with 1 ml of deionized water inside of the plastic tube. The mixture then undergoes sonification (Branson Ultrasonic 2800 bath) at 30 ° C for three minutes. As the Calix[4]arene powder was insoluble in water, it formed an inhomogeneous solution with an irregular shape of microcluster suspensions. Next, 20 µL of the sample was dropped using a micropipette onto a glass slide with double-sided tape on each side to produce a trapping chamber. The sample was then covered by a glass coverslip and sealed using nail polish. The illustration of the sample chamber is shown in Figure 2. The sample was then placed on the sample stage of the OT system for the optical trapping to take place. The trapping environment was maintained at 23°C.

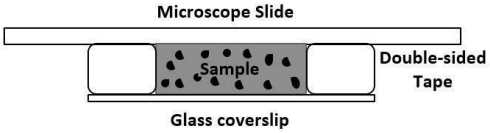

Figure 2. The illustration of the sample chamber.

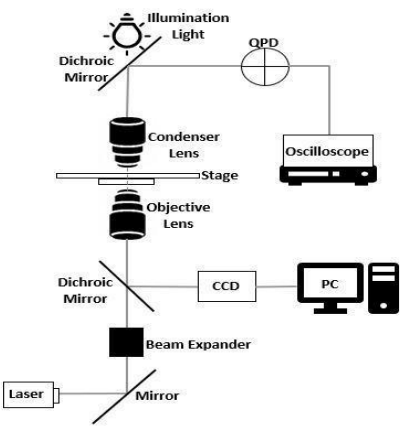

Figure 3. Schematic of the OT system setup.

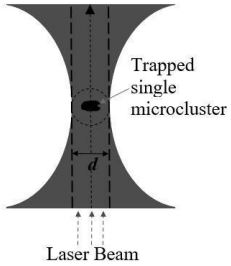

Figure 4. The illustration of a trapped microcluster inside a laser beam. *d* is the diameter of the laser beam.

In this study, we used a Modular Optical Tweezers instrument from Thorlabs. A schematic of the OT system that we used is shown in Figure 3. It consisted of a near-infrared laser (wavelength, λ = 976 nm) that passes through the beam expander. The beam entered the objective lens (Olympus, 100×, N.A 1.25, oil immersion) and focused into the sample chamber. The view of a single microcluster of Calix[4]arene trapping inside the focused laser beam is shown in Figure 4. The microcluster was trapped at the laser focal area, and *d* is the diameter of the laser power sport in this study (1.1 μm). The scattered laser beam was collected using a condenser lens (Olympus, 10×, N.A 0.25). The laser was reflected again by a dichroic mirror onto a quadrant photodiode, QPD (PDQ80A, Thorlabs), which detected the laser's intensity change and converted it into an electrical signal. The signal was then collected by an oscilloscope (Yokogawa, DL6054) connected to the QPD. The CCD camera captured images of the microcluster for visual observation.

Results and Discussion

When the sample chamber was placed onto the stage for optical trapping to take place, we actively seek for a single freely suspending microcluster that has the range of an effective radius between 0.5 to 3.0 μm within the camera view. Once a single microcluster was visible, the microcluster was temporarily held by tuning the optical power density of the laser, P, to 0.29 MW/cm^2. The microcluster was barely be trapped, but the condition was enough to measure the microcluster size in the xy plane of a single microcluster, as shown in Figure 5. It is essential to measure these perpendicular lengths because of the size irregularity of the microcluster. Equation (2) was used to determine the effective radius of a single microcluster by substituting the lengths. We were able to trap six microclusters of different sizes, as shown in Figure 6. After measuring the lengths, we pursued the experiment by increasing the laser power to 0.69 MW/cm^2. As a result, the optical trapping lasted longer than the previous laser power. We could move the microcluster around without 'dropping' it, indicating a stable trap was established. Therefore, $P_{lower} = 0.69$ MW/cm^2 was the lower limit for the laser power density for stable optical trapping from this observation. To find the upper limit of the optical power density, P_{upper}, we slowly increased the laser power while displacing the trapped microcluster in xy plane. This process continued until either the trapped microcluster could no longer move because it got stuck in the sample chamber wall or it gets pushed out of the laser focus. It happened because the laser power was too strong, causing the scattering force to increase and push the microcluster away from the laser focus and remained to the sample chamber's top wall. However, the value of the upper power limit of laser power density must be the value before the microcluster is propelled away from the laser focus. Table 1 below tabulated the upper power limit for six sizes of microcluster that we trapped in this study.

Table 1.

The upper power limit of laser power density for six sizes of microcluster to have stable optical trapping

.

l_x (μm)	l_y (μm)	$r*$ (μm)	P_{lower} (MW/cm2)	P_{upper} (MW/cm2)
1.0	1.0	0.5	0.69	2.67
njm	2.0	1.0		2.03
3.0	3.5	1.6		1.73
4.0	4.5	2.1		1.44
5.0	4.0	2.5		2.27
6.0	6.0	2.8		1.73

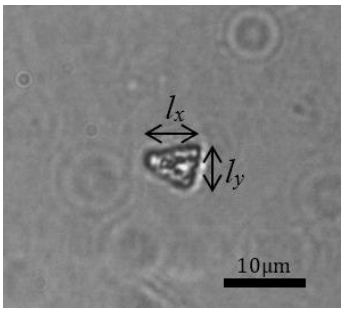

Figure 5. A single microcluster Calix[4]arene on the xy plane perpendicular to the laser beam direction.

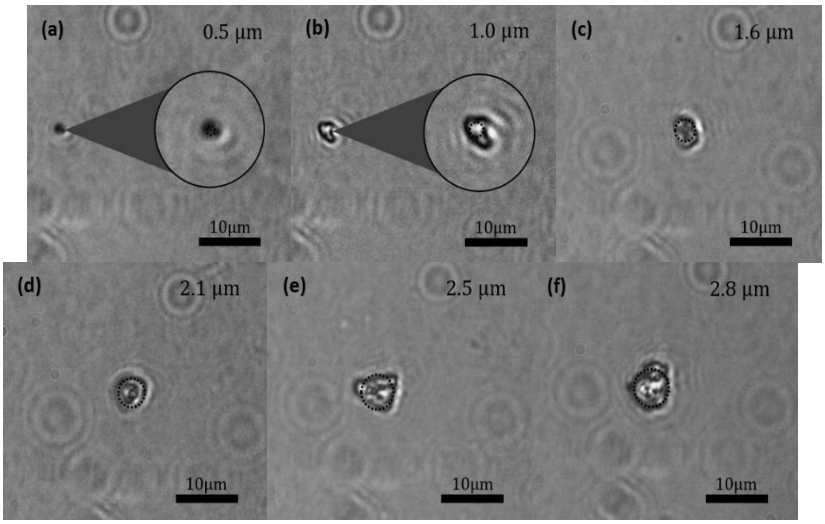

Figure 6. Images of six sizes of a single optically trapped microcluster of Calix[4]arene (a-f) in water were recorded with a CCD camera. Dotted line circles are eye guides for the effective radius r^*.

While the stable optical trapping of these single microclusters was achieved, the signal obtained from the QPD was collected and uploaded into the custom-made software (OSCal) [28] to analyze the f_c.

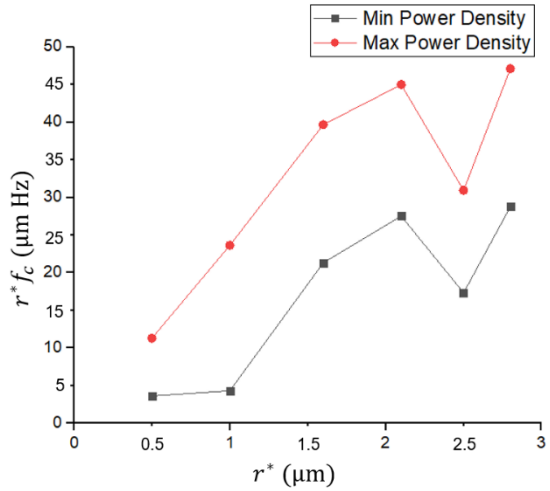

Figure 7. The product of the effective size and corner frequency, $r^* f_c$ versus the effective size of a single trapped microcluster of Calix[4]arene in water at the minimum and maximum power density.

f_c values were determined to evaluate the optical stiffness at the lower and upper power density limit to justify the stiffness of the trap. Supposedly the k_T should be stronger for higher power density, as long as the experienced gradient force is larger than the scattering force. Equation 1 can be approximated as $k_T = \beta r^* f_c$ where is the geometrical factor of the microcluster. Figure 7 shows the product of $r^* f_c$ versus r^*. We can immediately see that the optical stiffness increases with the microcluster size. As the larger microcluster was trapped, more parts of the laser light interact, contributing to the stronger gradient force. The effect of the gradient force is apparent for using upper laser power, P_{upper}. However, the optical stiffness was determined according to the microcluster trajectory in the xy plane as recorded by QPD. Even though the optical stiffness is stronger in the xy plane as the laser power density increases, it acts oppositely along the laser propagation direction. Along the z-axis, the scattering force becomes dominant proportional to the exerted laser power density [29]. The trap becomes unstable in this direction, and the microcluster gets pushed away easily. Figure 8 shows the upper and lower limit of the laser power density for stable trapping. Too low power was not enough to hold the microcluster, while overdense power density pushed away from the microcluster.

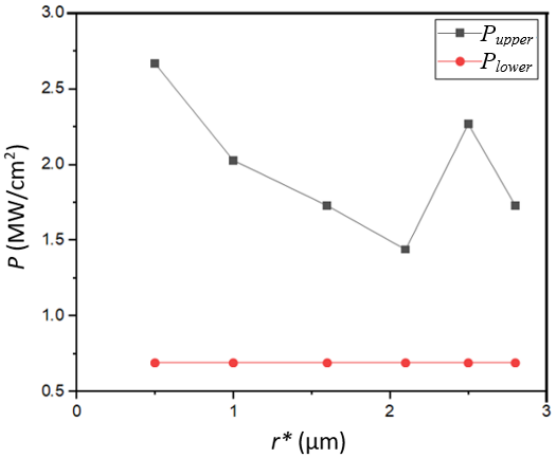

Figure 8. Power density, P, versus the effective size, r^*, of a single microcluster of Calix[4]arene in deionized water.

Conclusion

Based on the results from this study, we can conclude that the lowest limit of laser power density that we can set to have stable optical trapping regardless of any microcluster sizes was 0.69 MW/cm^2. In comparison, the upper power limit tends to decrease with microcluster sizes. The optical stiffness of the trap containing Calix[4]arene microcluster increase with its size. The results from this study may benefit more research in increasing the range of trapping possible in optical trapping. While it was challenging to justify the relation between microcluster size, optical stiffness, and the power limit, we have demonstrated that a microcluster of Calix[4]arene could be optically trapped despite the non-spherical and inhomogeneity of the microcluster. The finding provides a starting point for possible optically controlled calixarene microcluster for nanosensor applications in water.

Acknowledgements

This research has been carried out under the Fundamental Research Grants Scheme (FRGS/1/2017/STG02/UPSI/02/1) provided by the Ministry of Education of Malaysia and managed by RMIC, UPSI. The authors would like to extend their gratitude to Universiti Pendidikan Sultan Idris (UPSI) that helped manage the grants.

REFERENCES

1. Ashkin, A., *Atomic-beam deflection by resonance-radiation pressure.* Physical Review Letters, 1970. **25**(19): p. 1321.DOI: https://doi.org/10.1103/PhysRevLett.25.1321.
2. Suarez, R.A.B., A.A.R. Neves, and M.R.R. Gesualdi, *Optical trapping with non-diffracting Airy beams array using a holographic optical tweezers.* Optics & Laser Technology, 2021. **135**: p. 106678.DOI: https://doi.org/10.1016/j.optlastec.2020.106678.
3. X. J. Lv, et al., *"Evaporation of mixed citric acid/(NH4)2SO4/H2O particles: Volatility of organic aerosol by using optical tweezers," Spectrochim. Acta - Part A Mol. Biomol. Spectrosc., vol. 226, p. 117552,.* 2020.DOI: https://doi.org/10.1016/j.saa.2019.117552.
4. He, Q., et al., *Spectral-optical-tweezer-assisted fluorescence multiplexing system for QDs-encoded bead-array bioassay.* Biosensors and Bioelectronics, 2019. **129**: p. 107-117.DOI: https://doi.org/10.1016/j.bios.2019.01.004.
5. Konyshev, I., et al., *Force interactions between Yersiniae lipopolysaccharides and monoclonal antibodies: An optical tweezers study.* Journal of Biomechanics, 2020. **99**: p. 109504.DOI: https://doi.org/10.1016/j.jbiomech.2019.109504.
6. Hawes, C., et al., *Optical tweezers for the micromanipulation of plant cytoplasm and organelles.* Current opinion in plant biology, 2010. **13**(6): p. 731-735.DOI: https://doi.org/10.1016/j.pbi.2010.10.004.
7. Ma, G., et al., *Simultaneous, hybrid single-molecule method by optical tweezers and fluorescence.* Nanotechnology and Precision Engineering, 2019. **2**(4): p. 145-156.DOI: https://doi.org/10.1016/j.npe.2019.11.004.
8. Li, X. and D. Sun, *Automated transportation of microparticles in vivo*, in *Control Systems Design of Bio-Robotics and Bio-mechatronics with Advanced Applications*. 2020, Elsevier. p. 281-328.DOI: https://doi.org/10.1016/B978-0-12-817463-0.00010-1.
9. Kim, S., et al., *Controlled AFM manipulation of small nanoparticles and assembly of hybrid nanostructures.* Nanotechnology, 2011. **22**(11): p. 115301.DOI: https://doi.org/10.1088/0957-4484/22/11/115301.
10. Jauffred, L., et al., *Optical trapping of gold nanoparticles in air.* Nano letters, 2015. **15**(7): p. 4713-4719.DOI: https://doi.org/10.1021/acs.nanolett.5b01562.
11. Ashkin, A., *History of optical trapping and manipulation of small neutral particles, atoms, and molecules*, in *Single Molecule Spectroscopy*. 2001, Springer. p. 1-31.DOI: https://doi.org/10.1007/978-3-642-56544-1_1.
12. Yusof, M.F.M., et al., *Optical trapping of organic solvents in the form of microdroplets in water.* Chemical Physics Letters, 2020. **749**: p. 137407.DOI: https://doi.org/10.1016/j.cplett.2020.137407.
13. Nieminen, T.A. and N. R. Heckenberg, *"Laser trapping of non-spherical particles," pp. 304–307, 2000.* 2000.
14. Azmi, M.S.M., et al., *A Review of Calixarene Langmuir–Blodgett Thin Film Characteristics for Nanosensor Applications," Def. S T Tech. Bull., vol. 13, no. 2, pp. 205–216.* 2020.
15. Zhong, M.-C., Z.-Q. Wang, and Y.-M. Li, *Oscillations of absorbing particles at the water-air*

interface induced by laser tweezers. Optics Express, 2017. **25**(3): p. 2481-2488.DOI: https://doi.org/10.1364/OE.25.002481.
16. Zhu, R., et al., *Optical tweezers in studies of red blood cells.* Cells, 2020. **9**(3): p. 545.DOI: https://doi.org/10.3390/cells9030545.
17. Paul, A., P. Padmapriya, and V. Natarajan, *Diagnosis of malarial infection using change in properties of optically trapped red blood cells.* biomedical journal, 2017. **40**(2): p. 101-105.DOI: https://doi.org/10.1016/j.bj.2016.10.001.
18. Mondal, D. and D. Goswami, *Controlling local temperature in water using femtosecond optical tweezer.* Biomedical optics express, 2015. **6**(9): p. 3190-3196.DOI: https://doi.org/10.1364/BOE.6.003190.
19. Redding, B. and Y.-L. Pan, *Optical trap for both transparent and absorbing particles in air using a single shaped laser beam.* Optics Letters, 2015. **40**(12): p. 2798-2801.DOI: https://doi.org/10.1364/OL.40.002798.
20. Pan, Y.-L., S.C. Hill, and M. Coleman, *Photophoretic trapping of absorbing particles in air and measurement of their single-particle Raman spectra.* Optics express, 2012. **20**(5): p. 5325-5334.DOI: https://doi.org/10.1364/OE.20.005325.
21. Lin, J. and Y.-q. Li, *Optical trapping and rotation of airborne absorbing particles with a single focused laser beam.* Applied Physics Letters, 2014. **104**(10): p. 101909.DOI: https://doi.org/10.1063/1.4868542.
22. McGloin, D., et al., *Optical manipulation of airborne particles: techniques and applications.* Faraday Discussions, 2008. **137**: p. 335-350.DOI: https://doi.org/10.1039/B702153D.
23. Richard, W.B. and J.P. Miles, *Optical trapping and binding.* Rep. Prog. Phys, 2013. **76**(2): p. 026401.DOI: https://doi.org/10.1088/0034-4885/76/2/026401.
24. Gong, Z., et al., *Optical trapping and manipulation of single particles in air: Principles, technical details, and applications.* Journal of Quantitative Spectroscopy and Radiative Transfer, 2018. **214**: p. 94-119.DOI: https://doi.org/10.1016/j.jqsrt.2018.04.027.
25. Supian, F.L., et al., *Interaction between Langmuir and Langmuir− Blodgett films of two calix [4] arenes with aqueous copper and lithium ions.* Langmuir, 2010. **26**(13): p. 10906-10912.DOI: https://doi.org/10.1021/la100808r.
26. Anis, S., et al. *Behaviour of Composite Beam with Trapezoid Web Profiled Steel Section in Sub-Assemblage Frame*. Trans Tech Publ.DOI: https://doi.org/10.4028/www.scientific.net/AMR.250-253.1271.
27. Lim, D.C.K., F.L. Supian, and Y. Hamzah, *Langmuir, Raman, and electrical properties comparison of calixarene and calixarene-rGO using Langmuir Blodgett (LB) technique.* Journal of Materials Science: Materials in Electronics, 2020. **31**(21): p. 18487-18494.DOI: https://doi.org/10.1007/s10854-020-04392-6.
28. Hamid, M.Y. and S.K. Ayop, *LabVIEW-Based Software for Optical Stiffness Determination Using Boltzmann Statistics, Equipartition Theorem and Power Spectral Density Methods.* Advanced Science Letters, 2018. **24**(3): p. 1856-1860.DOI: https://doi.org/10.1166/asl.2018.11176.
29. Cuadros, J., et al., *Understanding optical trapping phenomena: a simulation for undergraduates.* IEEE Transactions on Education. Vol. 54, n. 1 (2011), p. 133-140, 2011.DOI: https://doi.org/10.1109/TE.2010.2047107.